

# Integration of Four-Dimensional Guidance with Total Energy Control System

Isaac Kaminer\* and Patrick O'Shaughnessy†  
Boeing Company, Seattle, Washington 98124

Presented here is a design of the four-dimensional mode for an integrated autopilot/autothrottle control system named Total Energy Control System. This design involves integrating a four-dimensional flight trajectory generator with the Total Energy Control System to create an outer-loop time error control law and integrating spoilers with the Total Energy Control System to increase the energy bleedoff capacity of the system during descent. The resulting system follows a precomputed four-dimensional profile in cruise, except if there is a large time error when the system is engaged. In such a case, the system generates a speed profile to null out the time error by the top of descent. During descent, the system follows a fixed profile by employing both throttles and spoilers. The system was tested on a full nonlinear simulation and all portions of the system were shown to perform as desired.

## Nomenclature

$a$	= flight-path acceleration limit
$D$	= airplane drag
$E$	= airplane energy
$\dot{E}$	= airplane energy rate
$\dot{E}_d$	= airplane energy distribution rate
$\dot{E}_s$	= airplane specific energy rate
$g$	= gravity
$h$	= airplane altitude
$\dot{h}$	= airplane vertical velocity
$h_c$	= altitude command
$\hat{h}_c$	= filtered altitude command
$K_{ei}$	= elevator command integral gain
$K_{ep}$	= elevator command proportional gain
$K_{ti}$	= thrust command integral gain
$K_{tp}$	= thrust command proportional gain
$q$	= dynamic pressure
$S$	= wing surface area
$s$	= complex frequency variable
$T$	= airplane thrust
$T_c$	= thrust command
$T_e$	= initial time error
$t_a$	= time to initiate speed change to meet $V_f$ constraint
$t_f$	= time to top of descent per four-dimensional profile
$t_{fl}$	= time to top of descent per four-dimensional profile under limit conditions
$V$	= airplane airspeed
$\dot{V}$	= airplane acceleration along flight path
$V_c$	= inertial speed command
$\hat{V}_c$	= filtered inertial speed command
$V_f$	= final ground speed per four-dimensional profile
$\dot{V}_i$	= inertial acceleration
$V_i$	= inertial velocity
$V_s$	= cruise speed
$V_t$	= true airspeed
$V_0$	= initial ground speed

$W$	= airplane weight
$w_n$	= natural frequency
$x_{crz}$	= cruise distance per four-dimensional profile
$x_{e0}$	= initial distance error
$x_f$	= $x_{crz} + x_{e0}$
$x_{fm}$	= maximum or minimum range possible
$\gamma$	= airplane flight-path angle
$\delta_{ec}$	= elevator command
$\delta_{spl}$	= spoiler position
$\delta_{splc}$	= spoiler command
$\delta_{tc}$	= throttle command
$\xi$	= damping ratio
$\tau$	= time constant

## Introduction

INCREASING air traffic congestion during the 1980s led NASA and leading airplane manufacturers to improve on time arrival at destination airports by intensifying research efforts in the area of four-dimensional profile generation and tracking. A great deal of work has been done by NASA, Boeing, Sperry, McDonnell-Douglas, etc., to develop on-board, real-time four-dimensional profile generation algorithms. Significant contributions in this area belong to Erzberger and Tobias<sup>1</sup> at NASA, Williams and Knox<sup>3</sup> at NASA, etc. This paper outlines the integration of Total Energy Control System (TECS) with the four-dimensional profile generator developed at Boeing.<sup>2</sup> The particular airplane used as a testbed for this design was the Boeing 737-100. (Although TECS is basically an outer-loop control system, it can be implemented on any transport airplane with minor modifications.)

There are several important issues that need to be resolved to successfully integrate TECS with the four-dimensional profile generator (Fig. 1):

1) The profile generated by the four-dimensional algorithm may have considerable discontinuities since the algorithm uses perturbation theory to simplify the aircraft equations of motion. This approach has inherent discontinuities between inner and outer solutions. For this application, the discontinuities will occur in speed and altitude profiles at transition points (i.e., climb to cruise, cruise to descent, and descent to bottom of descent at the metering fix). Therefore, the trajectory requires smoothing by introducing command processors that are driven by the four-dimensional profile and whose outputs are fed to TECS.

2) TECS must have a four-dimensional mode. In the four-dimensional mode, it should be able to null out any time errors

Presented as Paper 88-4067 at the AIAA Guidance, Navigation, and Control Conference, Minneapolis, MN, Aug. 15-17, 1988; received July 14, 1989; revision received March 13, 1990. Copyright © 1991 by the American Institute of Aeronautics and Astronautics, Inc. All rights reserved.

\*Research Engineer, Avionic Guidance and Control Research, Boeing Commercial Airplane Group; currently Graduate Student, Michigan State University, East Lansing, MI.

†Research Engineer, Avionic Guidance and Control Research, Boeing Commercial Airplane Group, Mail Stop 3T-AW.

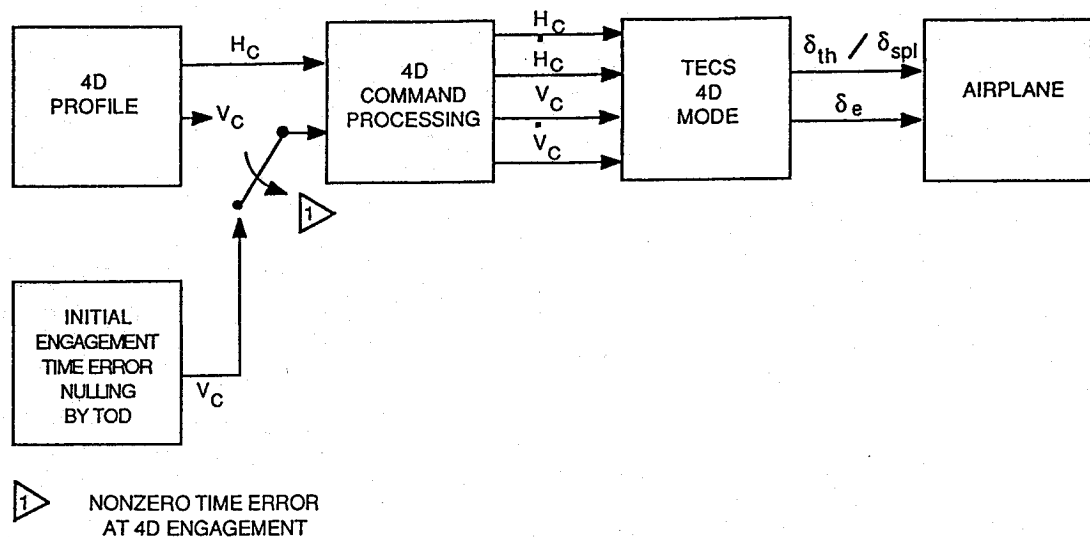


Fig. 1 General structure four-dimensional TECS system.

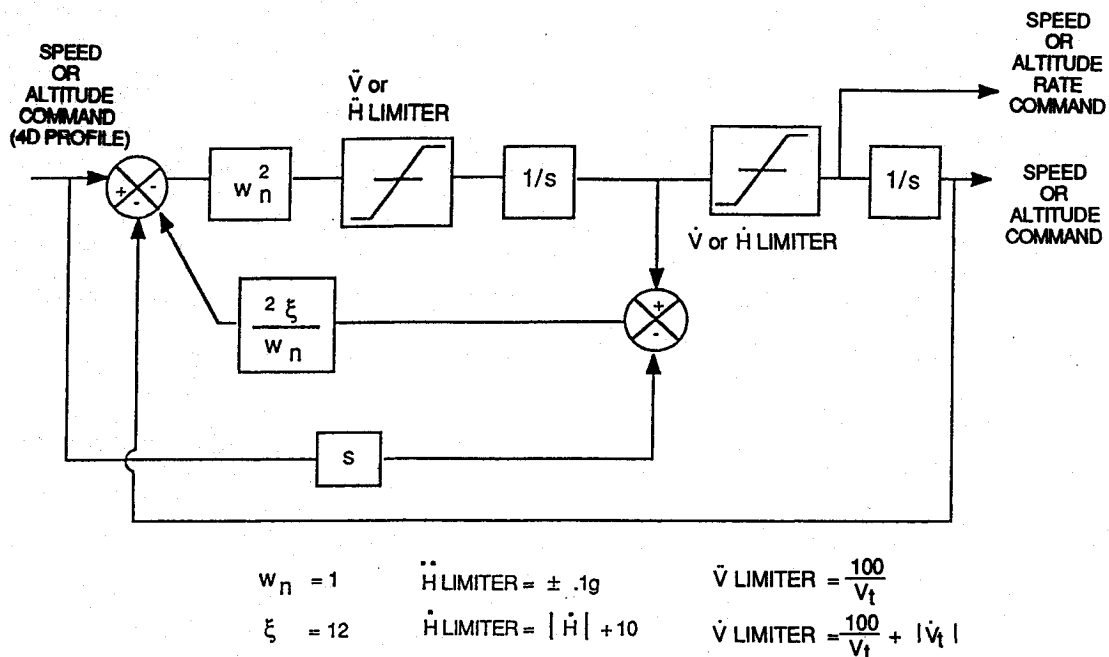


Fig. 2 Command processors.

to ensure timely arrival and also track speed and altitude profiles. Since the four-dimensional profile may have nonzero altitude rate and longitudinal acceleration commands, TECS should develop command errors based on both commands (altitude and speed) and rate commands (altitude rate and longitudinal acceleration).

3) In four-dimensional descent, the use of spoilers should be investigated to improve the trajectory tracking of the airplane when throttles are at idle.

#### Four-Dimensional Profile Smoothing

As previously mentioned, the four-dimensional profile generated by the optimal trajectory generator has significant discontinuities. This problem is corrected by filtering the profile with second-order filters, referred to here as command processors. The four-dimensional profile consists of altitude and speed commands as a function of time or distance. These commands are sent to TECS every 100 ms by the profile generator. Filtering, therefore, must be done on line. Figure 2 shows a diagram of the altitude and speed command proces-

sors. The following transfer function describes the input-output relationship of both processors:

$$\frac{\dot{V}_c}{V_c} = \frac{\dot{h}_c}{h_c} = \frac{w_n^2 [(2\xi/w_n)s + 1]}{s^2 + 2\xi w_n s + w_n^2} \quad (1)$$

The zero ( $w_n/2\xi$ ) in Eq. (1) is due to the feeding forward of the profile command rate, which provides tighter profile tracking by generating a lead term.

Command limiting is introduced to ensure passenger comfort ( $\ddot{H}$  and  $\ddot{V}$  limiters) and distribute energy between altitude and speed ( $\dot{V}$  limiter). The advantage of limiting before loop closure is the avoidance of undesirable stability effects that may be caused by the signal limiting inside the feedback loop. The command processors (Fig. 2) generate altitude rate and acceleration commands as required by the TECS four-dimensional mode. Here,  $w_n$  and  $\xi$  are set to 1 and 12, respectively.

#### Basic Concepts of Total Energy Control System

References 4-8 give a detailed discussion of TECS. However, since this paper describes the integration of spoilers into

TECS, a review of the design philosophy and theoretical concept of TECS is presented here, based on Ref. 7. TECS is an integrated autopilot/autothrottle system. The main objective of this system is to achieve decoupled altitude and speed response of the aircraft by coordinated control of elevator and throttles. The basic concept of TECS is to achieve total energy control of the airplane, which can be expressed as follows:

$$E = Wh + \frac{1}{2} \frac{W}{g} V^2 \quad (2)$$

The specific energy rate is given by

$$\dot{E}_s = \frac{\dot{E}}{W} = h + \frac{V\dot{V}}{g} \quad (3)$$

and normalizing by velocity

$$\frac{\dot{E}_s}{V} = \frac{h}{V} + \frac{\dot{V}}{g} = \gamma + \frac{\dot{V}}{g} \quad (4)$$

the acceleration of the airplane along the flight path for small values of flight-path angle (FPA) can be derived from the equations of motion for the airplane:

$$\dot{V} = g \frac{T-D}{W} - g\gamma \quad (5)$$

Substituting Eq. (5) for Eq. (4):

$$\frac{\dot{E}_s}{V} = \frac{T-D}{W} \quad (6)$$

Hence, any required changes in energy rate can be achieved by changes in  $T$  and  $D$ :

$$\frac{\Delta \dot{E}_s}{V} = \frac{\Delta(T-D)}{W} \quad (7)$$

Since the variation in the drag of the airplane for transports is slow, the change in drag in Eq. (7) is basically 0:

$$\Delta T_{\text{req}} = W \frac{\Delta \dot{E}_s}{V} \cong W \left( \Delta\gamma + \frac{\Delta \dot{V}}{g} \right) \quad (8)$$

Equation (8) indicates that the required thrust is directly proportional to the specific energy rate. Alternatively, it can be stated that the throttles control the rate at which energy is added to or deleted from the system.

Equation (8) can be used to develop the throttle control law, which converts the aircraft command errors into a specific energy rate error:

$$\frac{\dot{E}_{se}}{V} = \gamma_e + \frac{\dot{V}_e}{g} \quad (9)$$

where

$$\dot{V}_e = \frac{V_c - V}{\tau} - \dot{V} \quad (10)$$

and  $\gamma_e$  can be computed based on altitude error, FPA error, velocity control wheel steering (VCWS) angle command, or glide slope angle command. For instance, in the case of altitude error

$$\gamma_e = \frac{h_e}{V} = \frac{1}{V} \left( \frac{h_c - h}{\tau} - \dot{h} \right) \quad (11)$$

Based on Eqs. (8) and (11), the throttle control law takes the following form:

$$\delta_{tc} = K_{tp} \frac{\dot{E}_s}{V} + \frac{K_{ti}}{s} \cdot \frac{\dot{E}_{se}}{V} \quad (12)$$

However, achieving a speed maneuver without flight-path deviation, or vice versa, requires coordinated elevator and thrust responses. An energy rate distribution error can still exist (e.g., for too high a FPA and too low an acceleration). Correction of energy rate distribution error  $\dot{E}_{de}$  can be accomplished by taking a difference of potential and kinetic components of energy error:

$$\dot{E}_{de} = \frac{\dot{V}_e}{g} - \gamma_e \quad (13)$$

and, correspondingly, energy rate distribution:

$$\dot{E}_d = \gamma - \frac{\dot{V}}{g} \quad (14)$$

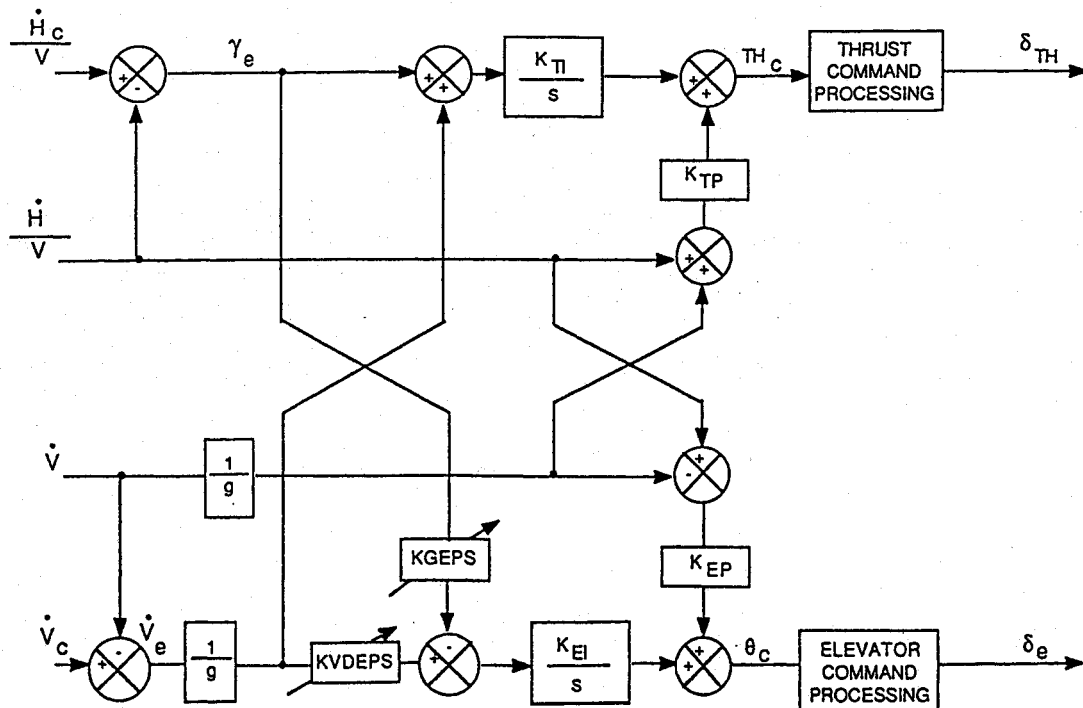
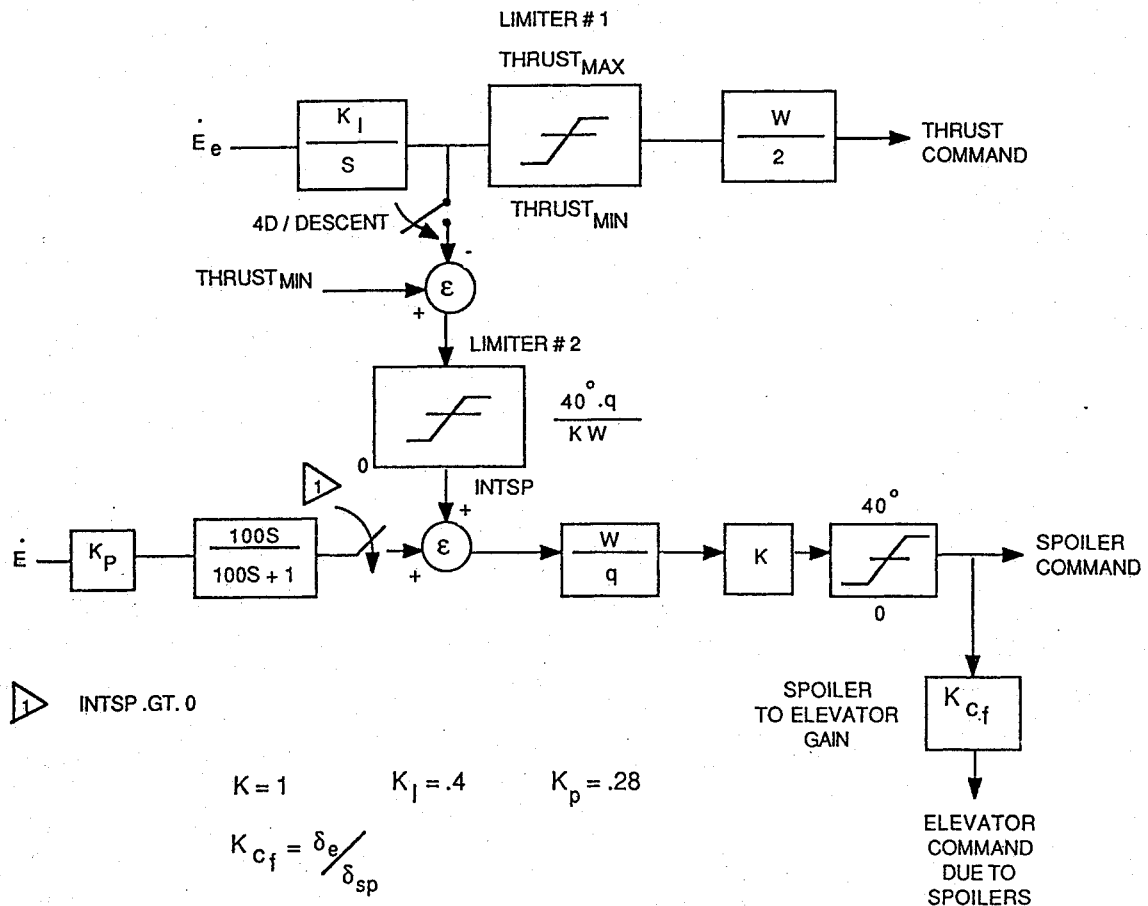
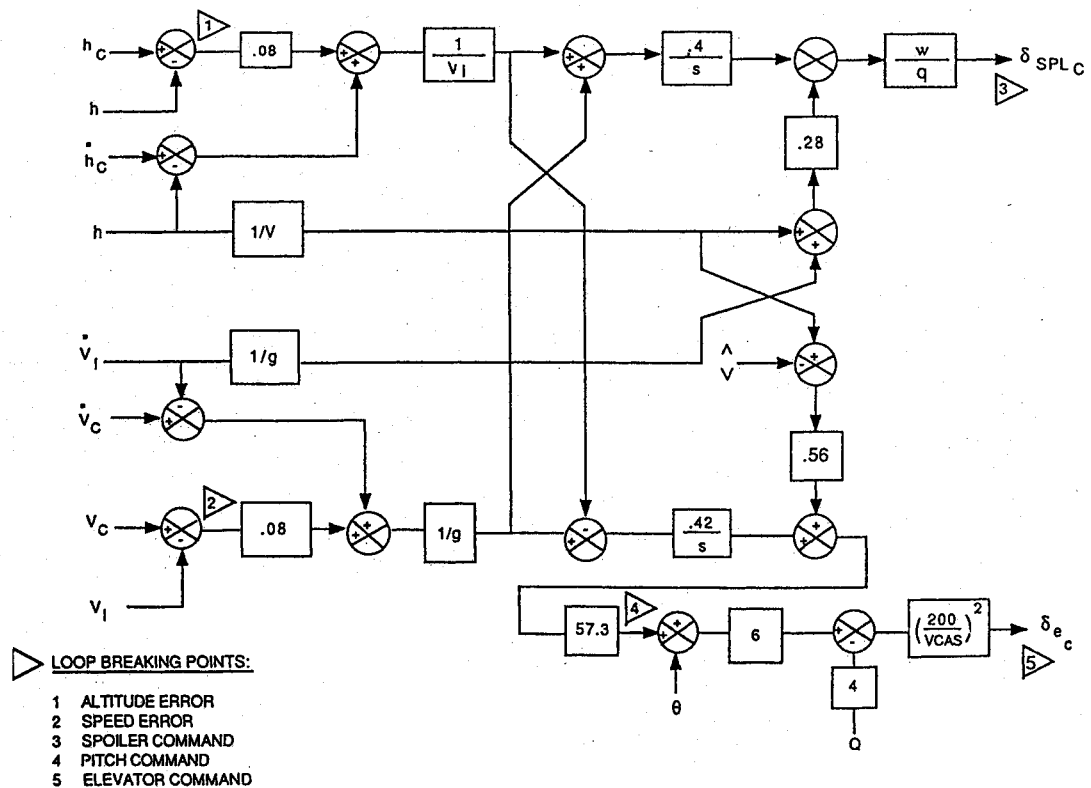


Fig. 3 TECS concept.



**Fig. 4 Spoiler command implementation.**



**Fig. 5 TECS spoiler configuration (linear model).**

Using proportional plus integral structure, the elevator control is

$$\delta_{ec} = K_{ep}\dot{E}_d + \frac{K_{ei}}{s}\dot{E}_{de} + \text{damping terms} \quad (15)$$

where damping terms consist of pitch and pitch rate feedback to ensure short period damping. This control law calls for the use of elevator to redistribute energy rate error  $\dot{E}_{de}$  between FPA and acceleration. This concept is shown in Fig. 3. Equations (12) and (15) are used to generate thrust and elevator commands, as well as spoiler command in four-dimensional descent, as will be described in the following section.

### Use of Spoilers in Four-Dimensional Descent

As mentioned in the previous section, TECS computes a throttle command based on specific energy error:

$$\frac{\dot{E}_{se}}{V} = \frac{T_{req}}{W} \quad (16)$$

This computation assumes a slow drag variation. This assumption is true, in general, unless a drag device is employed to increase the drag of the airplane. In such case, the drag term must be included in Eq. (16):

$$\frac{\dot{E}_{se}}{V} = \frac{T_{req} - D_{req}}{W} \quad (17)$$

Equation (17) represents a simple way of integrating spoilers into TECS. Additional energy must be taken out of the system (i.e., the spoilers should be deployed to increase drag to achieve the desired result) when the throttles are at idle ( $T = \text{const} = T_{min}$ ) during descent. Therefore, in Eq. (17), any change in  $\dot{E}_s$  will be caused by increased drag due to spoiler deflection:

$$\frac{\dot{E}_{se}}{V} \equiv \frac{-\Delta D_{\delta_{spl}}}{W} \quad (18)$$

where  $\Delta D_{\delta_{spl}}$  is the incremental drag due to spoiler deflection.

In terms of speed and altitude errors, Eq. (18) can be rewritten as follows:

$$\frac{\dot{E}_{se}}{V} = \left( \frac{h_c - h}{\tau} + \dot{h}_c - \dot{h} \right) \frac{1}{V} + \left( \frac{V_c - V}{\tau} + \dot{V}_c - \dot{V}_i \right) \frac{1}{g} \quad (19)$$

$$\Delta D_{\delta_{spl}} = q S C_{D_{\delta_{spl}}} \quad (20)$$

Assume  $C_{D_{\delta_{spl}}}$  is constant to get

$$\delta_{splc} \equiv K \cdot \frac{W}{q} \cdot \frac{\dot{E}_{se}}{V_i} \quad (21)$$

Equation (19) is a direct generalization of Eqs. (10) and (11). However, there are several important differences. Equation (19) uses  $\dot{V}_c$  and  $\dot{h}_c$ , which are generated by the command processors (see section on four-dimensional profile smoothing) and used as feed-forward commands to improve four-dimensional profile tracking. This is particularly important during transitions, and in climb and descent, when either  $\dot{h}_c$  or  $\dot{V}_c$  or both are nonzero. Also, Eq. (10) uses airspeed and true acceleration signals, whereas, Eq. (19) uses inertial ones. This difference is again due to the four-dimensional profile tracking application being solved. During descent, spoilers are used to bleed off excess inertial energy. Such situations occur most frequently when the airplane encounters tail winds. Thus, inertial speed and acceleration commands are used to compute both throttle and spoiler commands during four-dimensional descent.

To implement the spoiler command, an integrator is required to achieve zero steady-state energy error with a proportional path added to improve phugoid damping. Therefore, the spoiler command has the following form:

$$\delta_{splc} = \left[ \frac{K_I}{s} \dot{E}_{se} + K_p \dot{E}_s \right] \cdot K \frac{W}{q} \quad (22)$$

where  $K_I$ ,  $K_p$ , and  $K$  are gains to be determined by linear analysis. The PI (proportional + integral) structure in Eq. (22) is chosen in accordance with the PI structure already in TECS for the pitch command.

When compared with the thrust command definition in the previous section, it can be seen that the integral portion of the spoiler command is identical to that of the thrust command. Since the spoilers are used when the throttles are at the aft limit, the control logic, as shown in Fig. 4, was developed to engage spoilers automatically.

In Fig. 4, the thrust command is passed through a limiter (limiter 1), which restricts it to a normalized (divided by weight) maximum and minimum achievable thrust. Therefore, when the engines achieve the lower thrust limit, the output of limiter 2 becomes positive. This result triggers switch 1 to close and the spoiler command to be generated. The washout  $100s/(100s + 1)$  in the spoiler proportional path is necessary to prevent spoiler activity for a constant energy rate occurring in descent. Hence, the spoilers only react either to changes in commanded energy rate or to changes in inertial energy rate (e.g., due to winds).

Equation (22) shows the basic structure of the spoiler control law containing three gains  $K_I$ ,  $K_p$ , and  $K$  that should be determined by linear analysis. Initially  $K_I$  and  $K_p$  were set to 0.4 and 0.56 as in the original TECS design, where 0.4 is the value of the energy integrator gain and 0.56 is the value used in the proportional path for the pitch command. The value of  $K$  was selected to be 6 deg/rad to achieve the same crossover frequency in the spoiler command loop as in the pitch command loop (Fig. 5). Further investigation indicated that the value of 6 deg/rad is too high for  $K$  because it increases the crossover frequency in the speed loop (Fig. 5), which should be around 0.08 rad/s (12.5 s per original TECS requirements). To achieve the desired crossover in the speed loop, the value of  $K$  was decreased to 3 rad/s. The root locus analysis of the spoiler command proportional path loop showed that better damping of the short period mode can be achieved by reducing  $K_p$  to 0.28 (half of the original value). Therefore, gain values of 3, 0.28, and 0.4 for  $K$ ,  $K_p$ , and  $K_I$ , respectively, were used for nonlinear simulation testing.

During nonlinear simulation runs, lightly damped oscillations in the spoiler command were observed. When flight conditions used in nonlinear testing were analyzed for stability, it was found that the spoiler command crossover frequency was at 9 rad/s, compared with 2 rad/s for the nominal flight condition. The major difference between the nominal flight condition and the ones tested on the nonlinear simulation was the c.g. location, with 20% for the former and 10% for the latter. Therefore, to reduce excessive spoiler command bandwidth in the forward c.g. conditions, the value of gain  $K$  was reduced further to 1 deg/rad. This change did not effect the speed loop crossover a great deal, except in the extreme conditions, making it satisfactory for the final spoiler command configuration.

In the four-dimensional mode, the airplane follows an inertial trajectory. Therefore, as can be seen in Eq. (19), the inertial speed and acceleration are used to compute the spoiler command integral component. The spoiler command proportional path also uses inertial acceleration, thus making spoilers track purely an inertial path:

$$\delta_{splc} = \frac{0.4}{s} \dot{E}_{se} + 0.28 \dot{E}_s \quad (23)$$

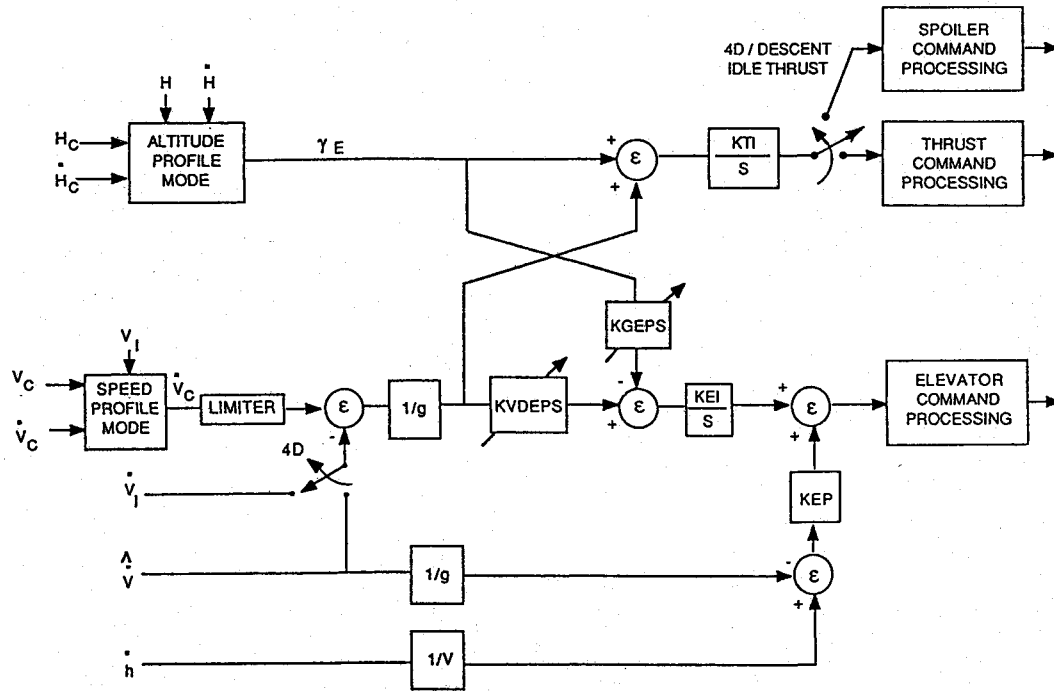
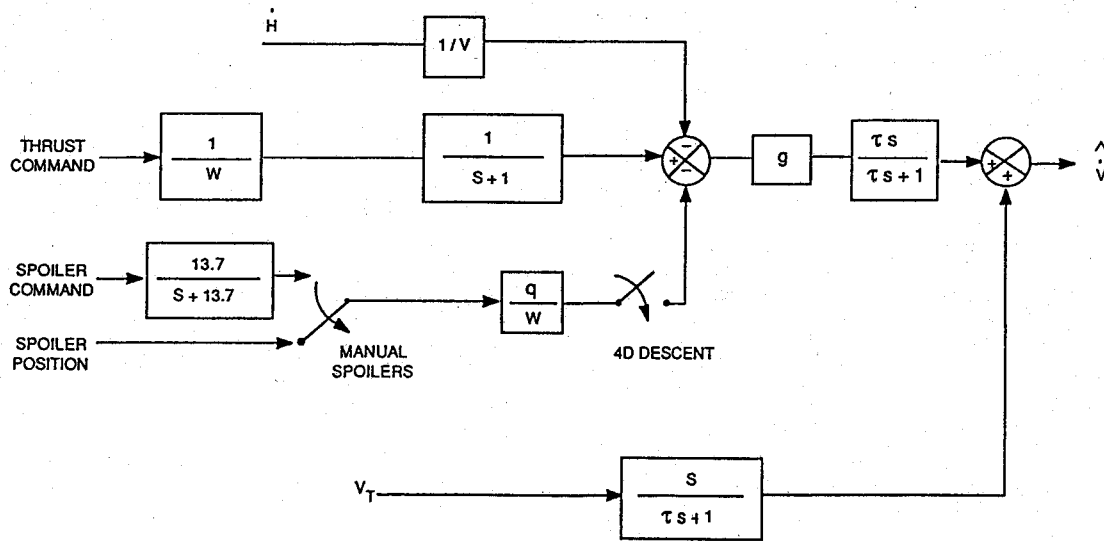


Fig. 6 Simplified TECS in four-dimensional mode.

Fig. 7  $\dot{V}$  filter.

where

$$\dot{E}_{se} = \frac{1}{V_i} \left( \frac{h_c - h}{\tau} + \dot{h}_c - \dot{h} \right) + \frac{1}{g} \left( \frac{V_c - V_i}{\tau} + \dot{V}_c - \dot{V}_i \right)$$

$$\dot{E}_s = \frac{\dot{V}_i}{g} + \frac{\dot{h}}{V_i}$$

The elevator command, on the other hand, uses inertial speed in the integral path and estimated air-mass acceleration in the proportional path:

$$\delta_{ec} = \frac{0.42}{s} \dot{E}_{de} + 0.56 \dot{E}_d \quad (24)$$

where

$$\dot{E}_{de} = \frac{1}{g} \left( \frac{V_c - V_i}{\tau} + \dot{V}_c - \dot{V}_i \right) - \frac{1}{V_i} \left( \frac{h_c - h}{\tau} + \dot{h}_c - \dot{h} \right)$$

$$\dot{E}_d = \frac{1}{V} \dot{h} - \frac{1}{g} \dot{\hat{V}}$$

This arrangement allows the elevator to track the air-mass energy distribution rate in the short term, thus minimizing the chance of stalling the airplane.

The decision to make spoilers control the inertial energy rate was based on linear time response analysis. Initially, it was decided that air-mass acceleration should be used for both spoiler and elevator commands, but analysis of the linear response to horizontal tail wind showed that the throttles came up first, followed by the spoilers. This kind of response is clearly undesirable. It was corrected by using the inertial acceleration in the integral paths for both the spoiler and elevator commands and in the proportional path for the spoiler command.

Spoiler deployment has a direct effect on the airplane pitching moment. Since lift is reduced aft of the spoilers on the wing, the airplane pitches up. This behavior may result in unnecessary elevator activity unless the elevator command can anticipate the change. A crossfeed from the spoiler command to the pitch command provided this anticipation, as shown in Fig. 4. The crossfeed gain  $K_{cf}$  is computed based on how much

elevator deflection is required to compensate for spoiler deflection. Its value is a function of altitude, Mach, and alpha and was derived using a least-squares curve fit to flight manual data.

In the four-dimensional mode, the inertial acceleration and speed are always used independent of whether throttles or spoilers are active (Fig. 6). In the case of throttles, this means that inertial instead of air-mass energy rate error is used to compute the throttle command (refer to the previous section).

TECS estimates the air-mass acceleration, based on the following formula:

$$\hat{V} = \frac{s}{\tau s + 1} V_t + \frac{\tau s}{\tau s + 1} g \left( \frac{T_c}{W} - \gamma \right) \quad (25)$$

In Eq. (25),  $\tau$  is a function of altitude. This formula assumes slow drag variation. Such an assumption is not valid when spoilers are deployed, hence, a drag term should be included in Eq. (25):

$$\hat{V} = \frac{s}{\tau s + 1} V_t + \frac{\tau s}{\tau s + 1} g \left( \frac{T_c - D_c}{W} - \gamma \right) \quad (26)$$

In Eq. (26)  $D_c$  is the drag due to spoilers estimated from the spoiler command:

$$D_c = \frac{13.7}{s + 13.7} \frac{W}{q} \delta_{splc} \quad (27)$$

$D_c$  is switched into the  $\hat{V}$  filter when the four-dimensional descent flag is set. Figure 7 shows a diagram of the  $\hat{V}$  filter with proposed changes.

### Initial Distance/Time Error Nulling

If there is a time error when the four-dimensional mode is engaged, it will be nulled by top of descent (TOD) (i.e., no time error nulling is to take place in the descent phase of the flight). To minimize throttle activity during the four-dimensional cruise, it is desirable to uniformly distribute time error reduction over the four-dimensional cruise. This task is successfully accomplished by the algorithm described in the following. Equations (28–30) describe the flight profiles. Without considering the speed limitations of the airplane, an analysis is performed to determine if a solution exists for the given constraints  $V_0$ ,  $V_f$ , and  $t_f$ . A simultaneous solution for  $X_{fm}$  yields Eq. (31). The value  $X_{fm}$  is the maximum range possible ( $a < 0$ ) or minimum range possible ( $a > 0$ ) for the given constraints. If the range that must be covered  $X_f$  falls within the maximum and minimum ranges, then a solution exists

$$V_s = V_0 + at_d \quad (28)$$

$$V_f = V_s - a(t_f - t_d) \quad (29)$$

$$X_f = \int_0^{t_d} (V_0 + at) dt + \int_{t_d}^{t_f} [V_s - a(t - t_d)] dt \quad (30)$$

$$X_{fm} = - (V_0^2 + V_f^2)/4a + V_0 V_f/2a + V_0 t_f/2 + V_f t_f/2 + at_f^2/4 \quad (31)$$

Should a solution not exist, then the final ground speed constraint  $V_f$  is met and a TOD arrival time error is computed and displayed. If a solution exists, then a ground speed profile is selected using elementary logic.

Once a ground speed profile has been selected, two unknowns must be determined. First, the necessary cruise speed  $V_s$  must be calculated. The second unknown is  $t_d$ . This is the time at which a deceleration/acceleration must be initiated to bring the ground speed of the airplane from  $V_s$  to the required

final ground speed  $V_f$ . These values are derived from the equations describing the selected ground speed profile.

The equations describing the profiles are

$$V_s = V_0 + at_1 \quad (32)$$

$$V_f = V_s \pm a(t_f - t_d) \quad (33)$$

$$X_f = \int_0^{t_1} (V_0 + at) dt + \int_{t_1}^{t_d} V_s dt + \int_{t_d}^{t_f} [V_s \pm a(t - t_d)] dt \quad (34)$$

which reduce to

$$V_s = \frac{1}{2}(at_f + V_0 + V_f) \pm \frac{1}{2}(a^2 t_f^2 + 2at_f V_0 + 2at_f V_f + 2V_0 V_f - V_f^2 - V_0^2 - 4aX_f)^{1/2} \quad (35)$$

$$V_s = [X_f + (V_0^2 - V_f^2)/2a]/[t_f + (V_0 - V_f)/a] \quad (36)$$

$$t_d = t_f + (V_f - V_s)/a \quad (37)$$

Implementing Eq. (37) results in TOD ground speed and arrival time errors when limit conditions hold the airplane actual ground speed  $V_{gs}$  at a value other than the desired  $V_s$ . To accommodate both the desired/unlimited ( $V_{gs} = V_s$ ) and limited ( $V_{gs} \neq V_s$ ) flight conditions, Eq. (37) is implemented as

$$t_d = t_f + (V_f - V_{gs})/a \quad (38)$$

This approach eliminates the final ground speed error (at the expense of a larger time error).

When throttles reach the set throttle authority limits or airspeed limiting occurs, the airplane is held at the corresponding ground speed. The resulting arrival time is

$$t_{fl} = (X_f/V_0) + (V_0/2a) + (V_f^2/2aV_0) - (V_f/a) \quad (39)$$

which is derived from

$$V_f = V_s - a(t_{fl} - t_d) \quad (40)$$

$$X_f = \int_0^{t_d} V_s dt + \int_{t_d}^{t_{fl}} [V_s - a(t - t_d)] dt \quad (41)$$

Under limit conditions, the airplane will be at a ground speed other than the desired cruise speed  $V_s$ . To meet the final ground speed constraint  $V_f$ , a new value of  $t_d$  must be generated:

$$t_d = t_{fl} + (V_{gs})/a \quad (42)$$

The corresponding TOD arrival error is

$$t_{ef} = t_{fl} - t_f$$

A TOD arrival time error message is displayed to the pilot.

### Altitude Profile and Speed Profile Modes

The smoothed four-dimensional altitude and speed profiles are fed to the TECS altitude and speed profile modes. Since the four-dimensional altitude speed profiles may contain nonzero acceleration and altitude rate commands, the corresponding TECS profile modes develop command errors from both position and rate commands.

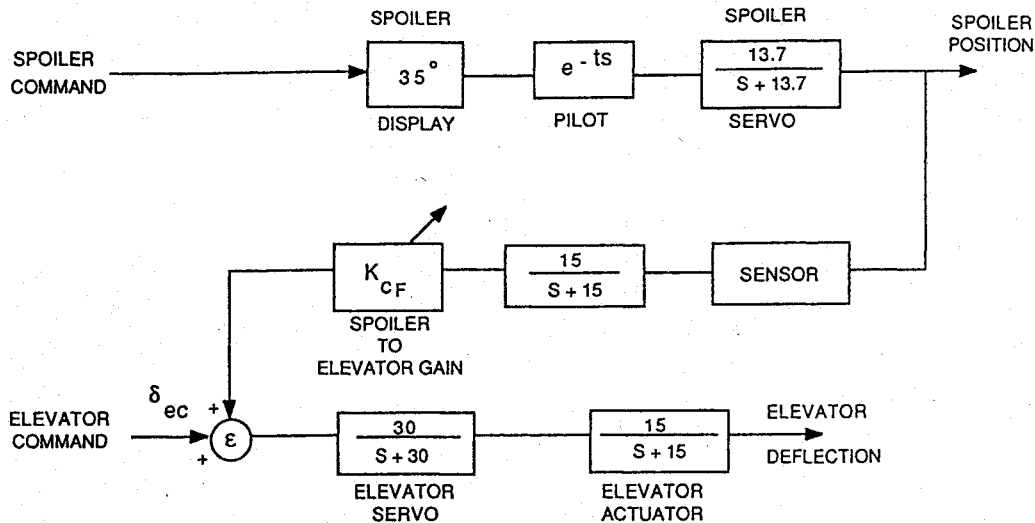


Fig. 8 Manual spoilers.

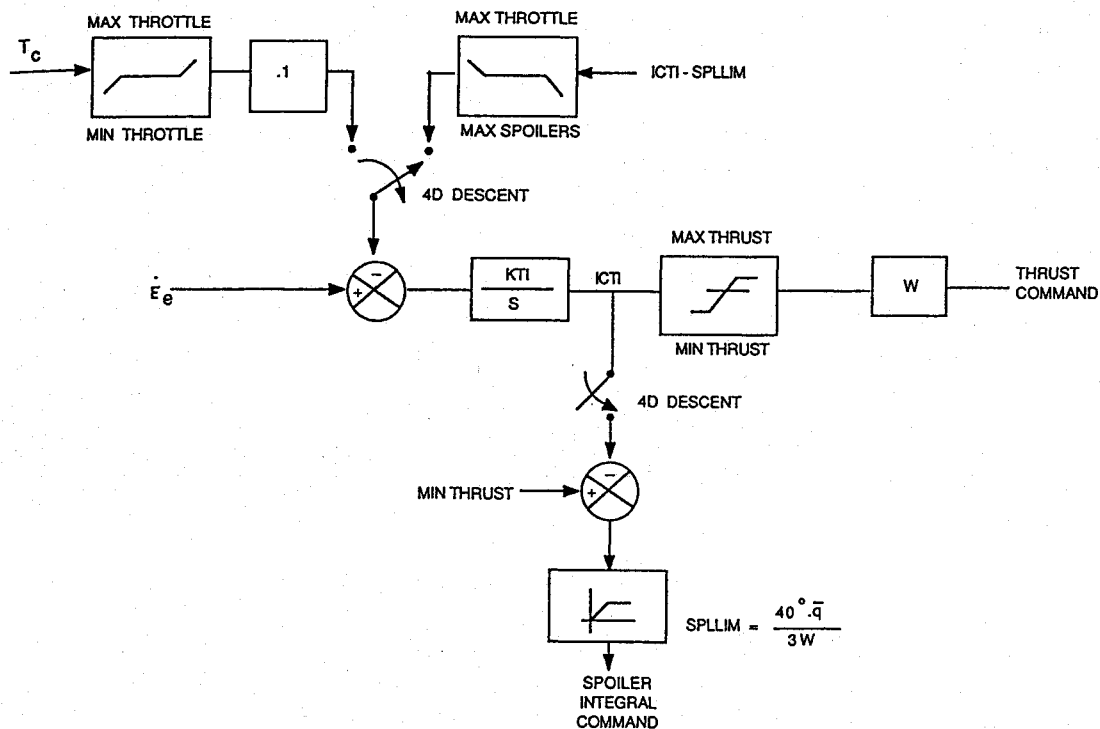


Fig. 9 Energy integrator limiting.

The altitude profile mode generates an inertial FPA error  $\gamma_e$  using the altitude command processor outputs  $h_c$  and  $\dot{h}_c$  ( $\dot{h}_c = 0$  when not in the four-dimensional mode):

$$\gamma_e = \left[ \left( \frac{h_c - h}{\tau} \right) + (h_c - h) \right] \frac{1}{V_i} \quad (43)$$

The speed profile mode generates an inertial acceleration error  $\dot{V}_e$  using the speed command processor outputs  $V_c$  and  $\dot{V}_c$  ( $\dot{V}_c = 0$  when not in the four-dimensional mode):

$$\dot{V}_e = \left[ \left( \frac{V_c - V_i}{\tau} \right) + (\dot{V}_c - \dot{V}_i) \right] \frac{1}{g} \quad (44)$$

### Manual Spoilers

Because of hardware constraints, the only way to control the spoilers on the NASA transport system research vehicle

(TSRV) airplane is by adjusting the speed-brake handle in the forward cockpit. Therefore, the automatic spoiler command is converted into a speed-brake setting advisory for the pilot, as shown in Fig. 8. The spoiler command bandwidth is low enough for the pilot to follow easily.

In the manual spoiler mode, the TECS structure reduces to speed on elevator for basic safety reasons (i.e., should the pilot choose not to deploy spoilers). However, the spoiler command remains coupled to the speed error and does not reduce to an altitude on spoiler mode. This configuration was found to reduce the magnitude of path deviations resulting from changes in pitch (i.e., the cross coupling of speed error to spoilers provides sufficient anticipation to allow the spoilers to remove altitude errors caused by changes in pitch as they occur).

Figure 8 also shows the spoiler position feedback to the elevator command required to retrim the aircraft in the manual spoiler mode. Spoiler to elevator gain is computed based



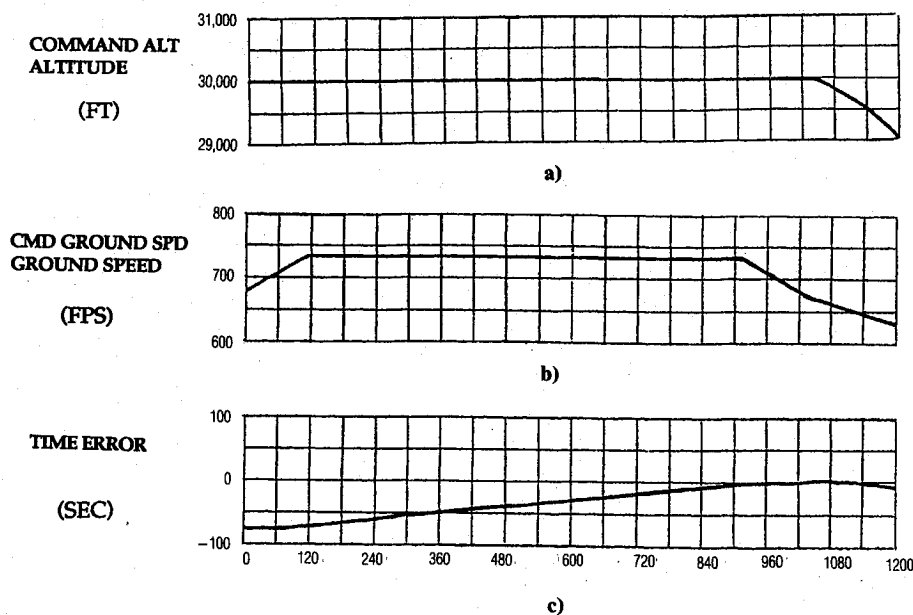


Fig. 10 Time error nulling in cruise.

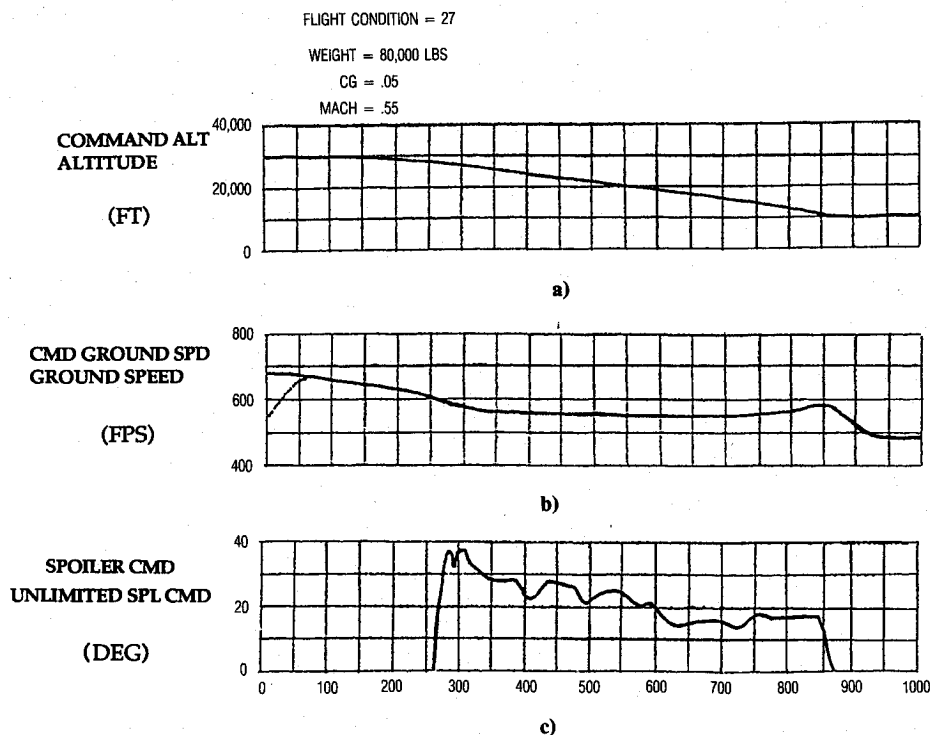


Fig. 11 Four-dimensional profile tracking in descent.

on how much elevator deflection is required to compensate for the pitching moment generated by the spoilers and is a function of altitude, Mach, and angle of attack. The system in Fig. 8 was analyzed for stability and found to be stable with sufficient phase and gain margins.

#### Four-Dimensional Mode Logic

To properly integrate the four-dimensional mode into TECS, new logic had to be added and some existing logic changed. The following new logic was added: 1) four-dimensional mode flag, 2) four-dimensional cruise flag, and 3) four-dimensional descent flag. The four-dimensional mode flag enables altitude and speed profile modes and spoilers in a four-dimensional descent. It also makes changes to existing logic, such as the AFTLIM flag definition and the energy integrator offloader logic.

The AFTLIM flag is set when throttles reach aft limit. This, in turn, forces the cross-coupling gain (KGEPS in Fig. 6) to zero and TECS into a speed on elevator configuration for speed priority modes. In four-dimensional descent, the spoilers are enabled, providing extended range for energy bleedoff. Therefore, the AFTLIM flag should not be set unless spoilers are at the limit in a four-dimensional descent.

The off-loader circuit is used to keep the energy integrator from saturating when throttles are at the limit. Since the same integrator drives the spoilers in a four-dimensional descent, it is necessary that the off-loader circuit not be turned on while the spoilers are active. This change is shown in Fig. 9. It should be noted that the off-loader circuit is a survivor of the analog days and can be replaced by simply turning off the integrator when either throttles or spoilers limit.

In the four-dimensional mode, the airplane tracks an inertial profile. Hence, when in the four-dimensional mode, iner-

tial acceleration is used to compute integral commands in both energy and energy distribution paths. The switch from the TECS estimated acceleration to the inertial one is accomplished when the four-dimensional flag is set. The four-dimensional cruise and the four-dimensional descent flags are to be provided with the four-dimensional flag. All three are enabled or disabled by the profile generator algorithm (PGA) or the flight management computer (FMC), whichever one is driving TECS in the four-dimensional mode. When the four-dimensional mode is disabled, the PGA or the FMC must select the next mode for TECS to fly and inform the pilot of the decision.

### Nonlinear Simulation Results

The TECS four-dimensional mode was implemented and tested on a nonlinear B-737 flight simulator. Figures 10 present the data for nulling out the time error in four-dimensional cruise with Fig. 10a showing an altitude profile that clearly indicates the top of descent point and Fig. 10b containing the speed profile computed by the algorithm and indicating the actual inertial speed of the airplane. As can be seen, both are identical. Figure 10c shows the estimated time error at the top of descent in which zero is clearly shown to be the top of descent point.

Figures 11 present the data for the descent portion of the four-dimensional flight. The airplane is subjected to tail wind that shears up to 50 kt at 1 kt/s 200 s into the descent. Figures 11a and 11b show that excellent altitude and speed profile tracking have been achieved in the presence of substantial tail wind. In both plots, the solid line indicates the command and the dashed line the corresponding airplane response. Figure 11c shows the spoiler activity in descent. The plots presented here testify to a successful design of four-dimensional mode for TECS. A more detailed analysis of the design can be found in Ref. 2.

### Conclusions

The integration of the four-dimensional profile generator with the Total Energy Control System has been developed and evaluated in detail. The feasibility of four-dimensional Total

Energy Control System integration has been demonstrated by meeting all design objectives in such a way as to minimize the volume of interface and mode switching logic. The design created a four-dimensional mode in the Total Energy Control System, which includes the following features:

- 1) Altitude and speed profile command processors to smooth out four-dimensional commands according to available airplane bandwidth and passenger comfort requirements.
- 2) Spoiler integration into the Total Energy Control System during four-dimensional descent.
- 3) Time error nulling algorithm to eliminate time error by top of descent.
- 4) Mode switching logic to allow for smooth integration of four-dimensional mode into the overall Total Energy Control System structure.

### References

- <sup>1</sup>Erzerberger, H., and Tobias, L., "A Time-Based Concept for Terminal-Area Traffic Management," *Proceedings of 1986 AGARD Conference No. 410, Efficient Conduct of Individual Flights and Air Traffic*, pp. 52-1-52-14.
- <sup>2</sup>Kaminer, I., and O'Shaughnessy, R., "4D-TECS Integration for NASA TCV Airplane," NASA Contract NAS1-18027, June 1989.
- <sup>3</sup>Williams, D. H., and Knox, C. E., "4D Descent Trajectory Generation Techniques Under Realistic Operating Conditions," AGARDograph AG-301, *Computation, Prediction and Control of Aircraft Trajectories*, 1987.
- <sup>4</sup>Lambregts, A. A., "Vertical Flightpath and Speed Control Autopilot Design Using Total Energy Principles," AIAA Paper 83-2239, Aug. 1983.
- <sup>5</sup>Lambregts, A. A., "Operation of the Integrated Vertical Flightpath and Speed Control System," Society of Automotive Engineers, Paper 831420, Oct. 1983.
- <sup>6</sup>Lambregts, A. A., "Integrated System Design for Flight and Propulsion Control Using Total Energy Principles," AIAA Paper 83-2561, Oct. 1983.
- <sup>7</sup>Bruce, K. R., Kelly, J. R., and Person, L. H., Jr., "NASA B737 Flight Test Results of the Total Energy Control System," AIAA Paper 86-2143, Aug. 1986.
- <sup>8</sup>Bruce, K. R., "Integrated Autopilot/Autothrottle Based on Total Energy Control Concept: Design and Evaluation of Additional Autopilot Modes," NASA Contract NAS 1-16300 and NASA CR-4131, April 1988.